Journal of Physics:
Conference Series

PAPER • **OPEN ACCESS**

Evaluation of turbulence characteristics in WRF simulations at WiValdi wind park

To cite this article: Gerard Kilroy *et al* 2024 *J. Phys.: Conf. Ser.* **2767** 052063

Journal of Physics: Conference Series **2767** (2024) 052063 doi:10.1088/1742-6596/2767/5/052063

Evaluation of turbulence characteristics in WRF simulations at WiValdi wind park

Gerard Kilroy, Antonia Englberger, Linus Wrba, Lukas Bührend, Norman Wildmann

[1]Deutsches Zentrum für Luft- und Raumfahrt, Institut für Physik der Atmosphäre, Oberpfaffenhofen, Germany

E-mail: gerard.kilroy@dlr.de

Abstract.

In this work we evaluate WRF-LES simulations at the WiValdi wind park at Krummendeich, North Germany. To accurately resolve fine-scale turbulence, we employ a high-resolution nested innermost grid with 5 m horizontal grid spacing. The main aim is to accurately reproduce realistic turbulent characteristics observed in neutral and stable atmospheric boundary layers. The so-called cell-perturbation method to accelerate the development of fine-scale three-dimensional turbulence is tested, and results are compared to in-situ observations and to another highly idealized numerical model running in LES mode.

While WRF without additional modifications is capable of reproducing the mean wind fields at the WiValdi wind park, it is unable to reproduce the turbulent characteristics observed. With the cell-perturbation method included, results are significantly improved, with turbulent characteristics much closer to observations.

Keywords: WRF-LES, neutral, stable boundary layer, turbulence, WiValdi, cell-perturbation method, EULAG

1. Introduction

Very recently, on 15.08.2023, the German Aerospace Center (DLR) with its partners of the research alliance wind energy Germany (FVWE) officially opened its research wind park (referred to as *WiValdi*) at Krummendeich, North Germany [1]. The wind park consists of two ∼4.3 MW wind turbines (WTs) which are placed in a row in line with the mean wind direction. A meteorological mast upstream and an array of three masts in between the turbines, combined with multiple Doppler wind lidars (DWL) and a microwave radiometer (MWR) will provide future studies of the wind park with a wealth of observational data with which to validate and improve high-resolution numerical model simulations designed to resolve turbulent features.

Previously, a version of the Weather Research and Forecasting (WRF) Model was validated during the intensive observation period (IOP) of the Perdigão field campaign by Wagner *et al.* [1] over complex terrain. WRF run in large-eddy simulation (LES) mode was shown to accurately simulate the observed mesoscale wind field over a long time period (1.5 months). The focus

[1] More information can be found on the official wind park website (www.windenergy-researchfarm.com).

of this study was to accurately represent the mesoscale flow over complex terrain, and not to simulate realistic turbulence which would require using higher horizontal resolution than used in their model setup. The authors suggested that they would possibly need 10 m grid spacing for stably stratified conditions, a requirement that would take a prohibitively long amount of time to simulate for the entire 1.5 month IOP. Another study of the Perdigão site by Wise *et al.* [2] found that the model is able to capture the observed behavior of the WT wakes, and they suggest that future studies could perform comparisons of modeled and observed turbulence quantities in the inflow fields. The ability to reproduce and forecast the inflow turbulent characteristics would be crucial for accurately estimating loads on the turbine itself, and for power production.

An aspect of the upstream atmospheric inflow is the stability of the atmosphere, with different environmental stabilities (neutral, stable, or convective) associated with markedly different environmental turbulent structure. Different environmental stabilities affect also properties of the near and far wake produced by a turbine. Whereas under convective conditions, the wake recovers very rapidly, the streamwise wake extension is much more relevant for a waked turbine in shear-driven atmospheric situations like neutral or stably-stratified cases. The wake-turbine interaction is a major contribution to loads in wind parks and plays a major role for park efficiency. Wind speed deficit and turbulence in the wake has therefore been intensively investigated in idealized modeling studies [3, 4, 5].

It is vital to assess the ability of numerical models to accurately simulate the background inflow conditions before moving on to more complex simulations employing turbine paramaterizations and assessing wake effects [6]. One particular issue with accurately simulating the inflow conditions is that numerical models are often driven by low-resolution weather data used for initial and boundary conditions. In WRF, lateral boundary information is passed from outer domain to inner domain, a mesoscale-to-microscale coupling, with the outermost domain typically driven by global weather model analyses. In the transition from a mesoscale domain to a microscale domain, the boundary conditions supplied are interpolated from the resolution of the lower-resolution mesoscale model, and therefore are initially too smooth at the inflow edges (a result of transitioning from a 1D planetary boundary layer scheme to LES closures). A recent review paper which focuses on advances in mesoscale to microscale modeling highlights some of these issues [7]. To develop realistic fine-scale turbulent features in WRF at the location of interest, a relatively large fetch is required. Typically, turbulence in LES domains is generated through a combination of friction, momentum and heat mixing, heat fluxes from the surface, complex topographical features, or variable land cover including forests.

The WiValdi wind park is topographically very simple, with flat low-lying terrain, and has little in terms of large-scale woodland or other complex land-usage features. This means that if the inner LES domain is too small, and the wind speeds relatively large, it is possible that turbulence does not manifest in shear-driven situations and calculations of power generation and turbine-wake interactions would be inadequate. To this end, the so-called cell perturbation method (CPM) was developed over the last decade [8, 9, 10]. This method provides the ability to develop realistic small scale turbulence without the need for prohibitively long fetches by introducing stochastic temperature perturbations at the LES inflow boundaries. These temperature perturbations trigger small scale vertical motions that produce complex small-scale horizontal vortical motions. It was shown by the authors above that this method "significantly accelerates the generation of realistic turbulence". The method also adds energy to turbulent spectra at higher frequencies.

Here, we evaluate WRF simulations of the WiValdi wind park in LES mode using CPM against on-site observations. To accurately resolve fine-scale turbulence, we employ a high-resolution nested innermost grid with 5 m horizontal grid spacing. This work aims to evaluate the ability of WRF-LES to accurately reproduce realistic turbulent characteristics in a neutral and stable atmospheric boundary layer (ABL), with the future goal of accurately representing

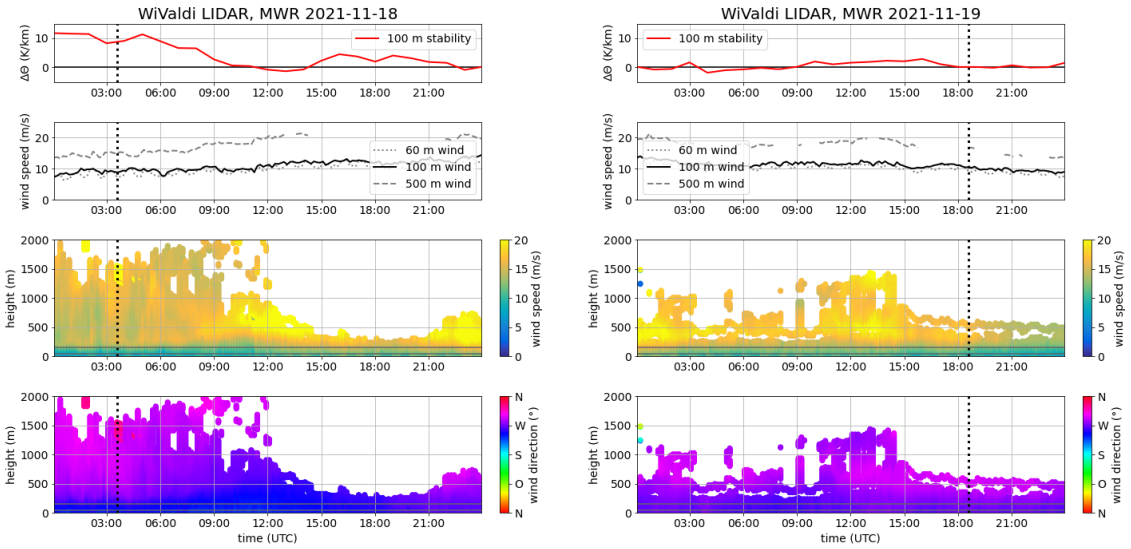

Figure 1. DWL and MWR observations for the stable case on 18.11.2021 (left) and the neutral case on 19.11.2021 (right). The top two panels show time-series of potential temperature stratification at a height of 100 m, and wind speed at various heights, middle panels show wind speed, and bottom panels show wind direction. A dashed black line highlights the time of interest during both days.

also convective ABLs, and other atypical high-load weather events such as low-level jets, winter storms and convective cold pool events. The validation of the ability of WRF to produce realistic turbulence for WiValdi is important as models can provide information at much higher temporal and spatial resolution than observations alone, allowing for more accurate load calculations on turbines and energy output estimates.

2. Methodology

2.1. Observations

From November 2020, a DWL along with a MWR have been in operation at the WiValdi site, in order to provide a climatology of the dynamic and thermodynamic situation. The DWL is operating in a velocity azimuth display (VAD) mode with a high angular resolution and a specific elevation angle in order to obtain measurements of, for example, the wind field and TKE. The MWR measures vertical profiles of temperature and humidity. An analysis of the long term statistics (16 months of data) has been published [11]. Quantities such as TKE are produced from time-averaged fields over a period of 30 minutes, and are available once every hour.

Two real scenarios are simulated in this study, a quasi-stable case and a quasi-neutral case. Figure 1 shows DWL and MWR observations, stability, wind speed and direction, for both of these chosen days. Characteristic profiles of neutral and stable boundary layers for the Krummendeich site were identified from DWL and MWR data. A particular day (19.11.2021) for the neutral case was chosen as it contained neutral stratification (stability values close to 0 K km^{-1}) in the boundary layer for relatively long periods during the day (Fig. 1, top panel), wind speeds close to the nominal wind speed of the WT at hub height (10 m s^{-1}), and the wind direction was such that the wake from the first WT would interact with the second downstream WT. Note that, at the WiValdi site in 2021, no WTs had yet been built and we do not include a WT paramaterizations in the model code. The aim of the current work is to assess the ability of WRF to reproduce the environmental inflow fields at the site WiValdi, with the caveat that

the current setup can be used in future studies that include wind turbine paramaterizations to study turbine wake characteristics. The sonic anemometer on the wind mast started to provide data from November 2022, and therefore cannot be used in this study to validate the model.

A stable case was identified on 18.11.2021, which had similar hub height wind speed and wind direction as the neutral case. The night time period was particularly stable, with values of around 10 K km^{-1} occurring between 00 UTC and 06 UTC.

2.2. WRF

The simulations presented herein are performed by WRF V4.4.1, a state-of-the-art non-hydrostatic model used frequently in the community for both operational and research applications [12]. The model integrates the fully compressible Euler equations on a terrain following hybrid, sigma-pressure vertical coordinate. A major advantage of the WRF model is that it has the capability to run simulations at the microscale level in LES mode, where larger turbulent features are explicitly resolved. Through nesting, mesoscale domains using a 1D planetary boundary layer scheme provide lateral boundary conditions to the LES domains.

The numerical model set-up consists of 5 nested model domains with horizontal resolutions of 5, 1, 0.2, 0.04 and 0.005 km, respectively. The number of horizontal grid points of the domains are 300x300, 251x251, 251x251, 251x251 and 473x353 for the respective domains 1 to 5. In the stable case simulation the inner domain (D5) has more grid points in the x-direction, namely 601x353. In the vertical direction 95 grid points are used in the innermost domain (D05). Vertical nesting is applied also, so that higher vertical resolution is used in the domains with higher horizontal resolution. In domain 5, the lowest model levels are 5, 15, 25 and 40 m above ground level. Domain 5 is the focus of the current work.

Initial and boundary conditions are provided by European Centre for Medium-Range Weather Forecasts (ECMWF) operational analyses, which are available every 6 h. The three innermost domains are performed in LES mode. The high resolution of the innermost domains requires the usage of higher resolved topography and landuse data than supplied originally in WRF. To that effect the COPERNICUS digital elevation model (90 or 30 m resolution) and the CORINE land cover (CLC) data are applied.

The model top was set at 12 km height to include tropopause effects. A 3 km upper damping layer is implemented, to restrict reflection of gravity waves. A Revised MM5 Monin-Obukhov scheme is used to simulate the surface layer [13]. Additionally, the Noah-MP land surface model [14], the Rapid Radiative Transfer Model long-wave scheme [15], the Dudhia short-wave scheme [16], the WRF single-moment five-class microphysics scheme [17] are used. In domains 1 and 2 the Kain–Fritsch cumulus paramaterizations scheme is implemented [18]. In the LES domains (domains 3-5) the cumulus parameterization is switched off. For all domains a relatively new 3D TKE subgrid mixing scheme that is self-adaptive to the grid size between the LES and mesoscale is utilized [19]. The cell perturbation method is applied to all LES domains.

The simulations for the neutral case were performed for a total of 7 hours, from 12 UTC to 19 UTC on 19.11.2021. The first 6 hours in this simulation are considered as model spin up. A longer spin up time for the outer domains in the stable case was implemented, with domains 1-4 initializing at 00 UTC on 17.11.2021, and domain 5 initializing a day later on 18.11.2021. For the neutral case a total of two simulations are analyzed here and compared to observations. One simulation includes the CPM to accelerate the flow towards a turbulent state, while the other does not. For the stable case, only one simulation with the CPM was performed. All simulations are compared to observational data, when available, and to output from another idealized model (described below).

Due to the idealized model (described below) simulating the environmental conditions only at a specific time (a chosen observed profile), it is possible to only make comparisons to both observations and the idealized model together for a relatively limited time window. To this

extent, a relatively short period of WRF output has been chosen to be the focus of this study. A time range of 18:30 - 18:34 UTC on 19.11.2021 was chosen to be the focus for the neutral case. A period at around 03:35 UTC was identified as being notably stably stratified and will be the focus for the stable case (see dashed lines in Fig. 1).

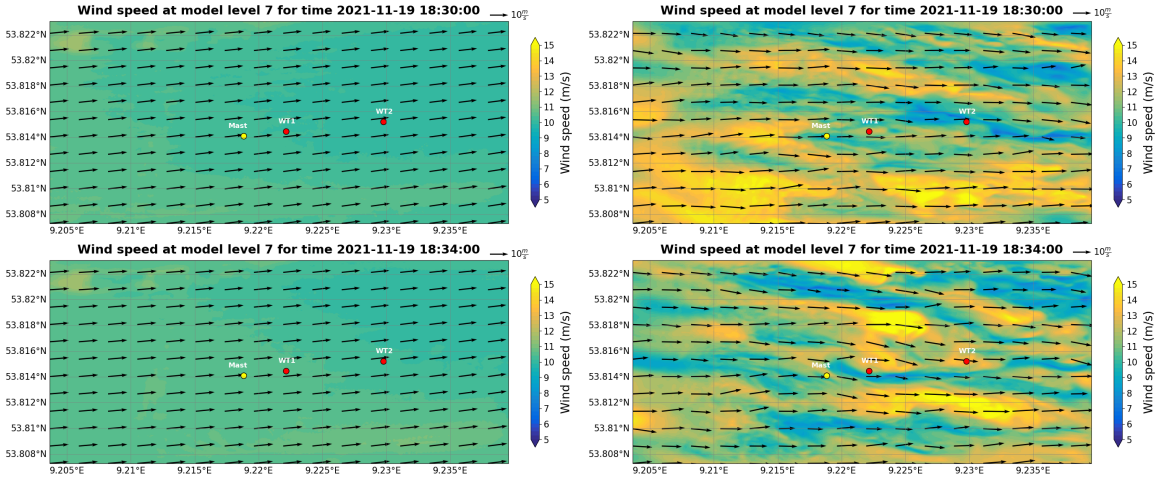

Figure 2. Horizontal cross sections of wind speed at model level 7 (approximately 100 m height) at 18:30 UTC (top panels) and 18:34 UTC (bottom panels). The left panels are for WRF_noCPM_n, right panels for WRF_CPM_n. Highlighted are the locations of the inflow measurement mast (yellow dot) and the two turbines (red dots, labeled WT1, WT2).

2.3. EULAG

Both considered atmospheric regimes, the near-neutral as well as the stably-stratified situation are in addition simulated with the numerical model EULAG [20]. EULAG is well suited for idealized LESs, but it also has the ability to assimilate to measured mean profiles [21, 22].

EULAG solves the Boussinesq equations for incompressible atmospheric flow for the Cartesian velocity components and the potential temperature perturbation. The equations include viscous dissipation of momentum and heat. The implemented subgrid-scale model uses a TKE closure taking into account the stability limited vertical diffusion combined with an anisotropy model, which is especially important during night-time situations, as it considers the turbulence length scale reduction near the surface.

The simulations of both stratification types require a precursor simulation of the corresponding regime and an assimilation simulation which performs a type of meso-microscale coupling. The model adapts mean velocity profiles to measured profiles via an additional forcing term in the u and v-components of the Boussinesq equations, while the turbulence structure of the precursor simulation is preserved (with modifications related to the additional forcing term to adapt mean profiles). The precursor simulation of the near-neutral stratification is driven by a pressure gradient, whereas the stably-stratified regime is driven by the Coriolis force. Surface cooling is performed with Neumann boundary conditions. Whereas the near-neutral case uses a grid spacing of 5 m in each direction, it is refined down to 3 m in the stable case. EULAG simulations are used as an additional tool to assess the ability of WRF to generate turbulence when compared to a highly idealized model, particularly in regions where observations don't exist.

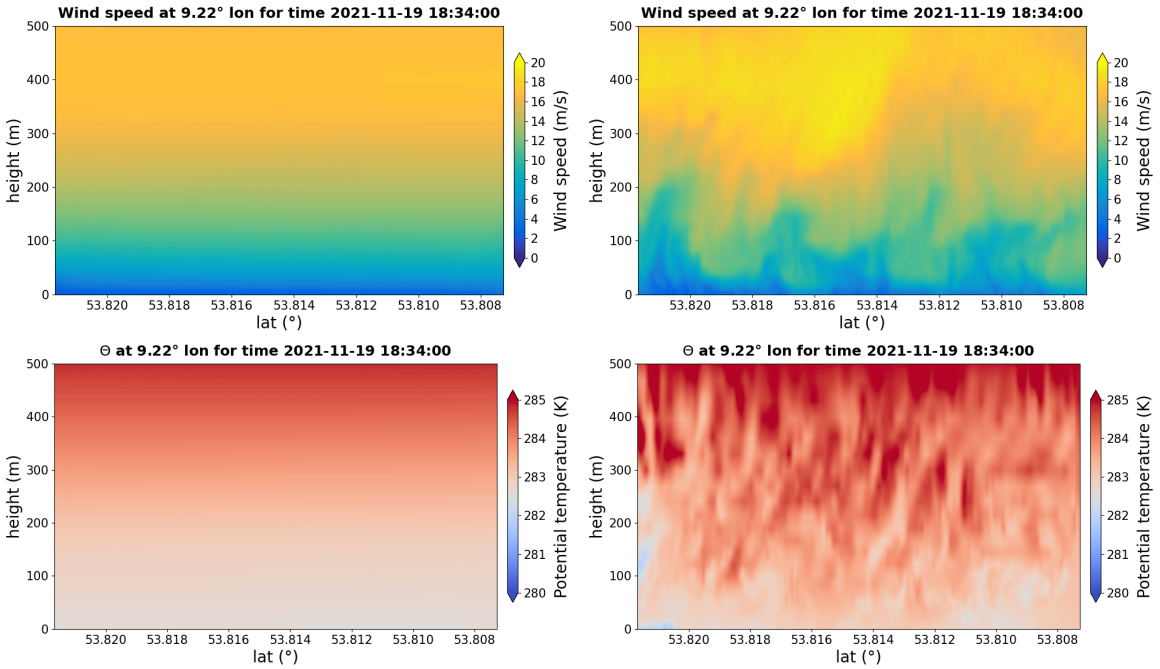

Figure 3. Vertical (north-south) cross sections of wind speed (top panels) and potential temperature (bottom panels) through the location of first wind turbine (WT1) up to 500 m height at 18:34 UTC. The left panels are for WRF_noCPM_n, right panels for WRF_CPM_n.

The two EULAG simulations presented herein are described in more detail in recent publications. The neutral case is presented in a paper which compares a Newtonian relaxation technique and a vibration assimilation method in order to determine the most efficient method to compute realistic inflow fields for wind-turbine simulations [21], while the stable case is presented as a component in a simulation tool-chain which reproduces characteristic turbulence of the stably-stratified ABL [22].

3. Results

The focus is initially on the neutral case, where we compare a WRF simulation with (hereafter WRF_CPM_n) and without the CPM (hereafter WRF_noCPM_n) with on-site observations. In addition to the two WRF simulations, an extra simulation using EULAG (hereafter EULAG_n) is included in the analysis. This simulation assimilates the mean profile of a precursor EULAG simulation towards the vertical profiles of u and v at the wind park [21]. The model setup in EULAG is more idealized than in WRF, however, comparison with measurements show the generation of suitable atmospheric inflows for wind-turbine simulations [21, 22].

3.1. Neutral case

To begin the analysis, it is worth presenting horizontal snapshots of the flow which qualitatively show whether or not the flow is turbulent. In Figure 2, horizontal cross sections of wind speed close to 100 m height (slightly above hub height of the wind turbines in WiValdi) for the two times are shown. The left panels show WRF_noCPM_n, right panels WRF_CPM_n. It is clear to see that the flow in WRF_noCPM_n has very low turbulence, with only very small deviations to the mean flow. The situation does not change over time, and 4 min later the flow is essentially the same. For WRF_CPM_n (right panels) the flow is much more turbulent with wind gusts and other coherent turbulent structures occurring. These structures are highly

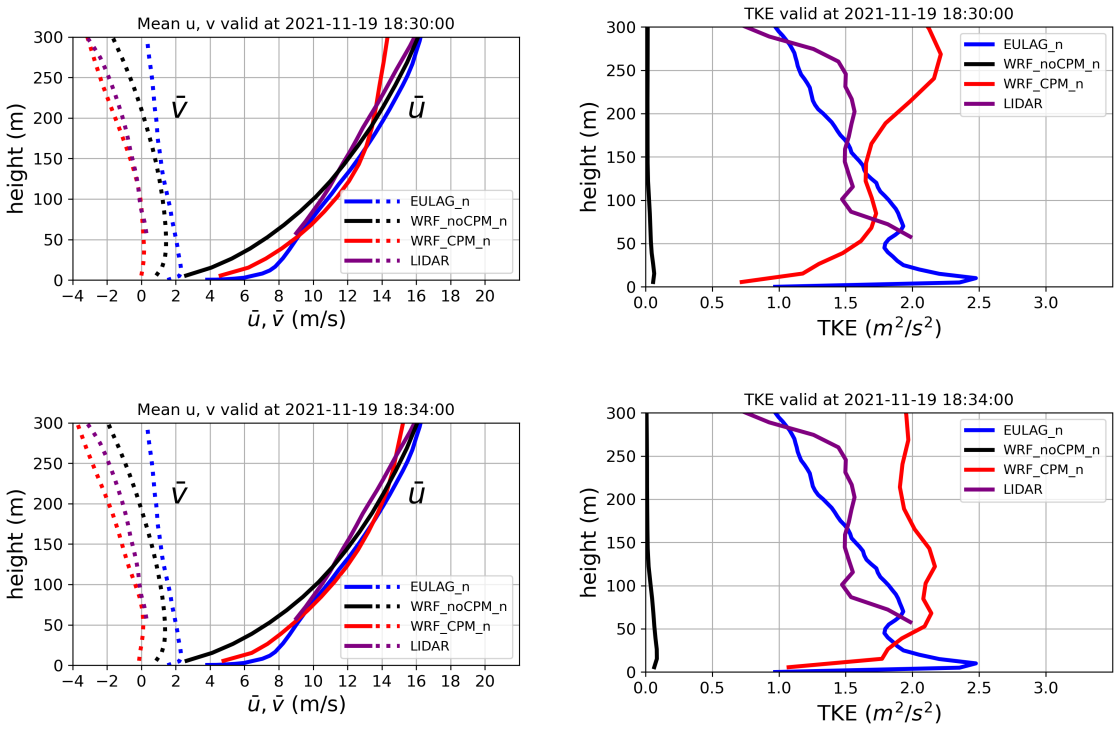

Figure 4. Horizontally averaged (up to 300 m height) zonal (solid curves) and meridional (dashed curves) velocity (left panels) and TKE (right panels) for 18:30 UTC (top panels) and 18:34 UTC (bottom panels). The method used in the calculation of TKE from DWL data is described in [11].

variable in time and the flow field is quite different only 4 min later. Figure 3 shows vertical cross sections up to 500 m height at 18:34 UTC for both WRF simulations. Both the wind speed and potential temperature fields are shown. As expected, the fields are much less turbulent also in the vertical in WRF_noCPM_n. In WRF_CPM_n the fields are clearly more turbulent and appear more realistic. The next step is to quantify the turbulent fields shown here and compare to observations and EULAG results.

Figure 4 shows horizontally-averaged[2] variables to a height of 300 m for the two WRF simulations, for the EULAG simulation as described above, and the closest observations in time recorded at the wind park. The left panels show the mean horizontal flow, while the right panels show TKE (where TKE is given by $\frac{1}{2}(\sigma_u^2 + \sigma_v^2 + \sigma_w^2)$, and σ refers to the variance of the given wind component). While, qualitatively, the turbulent features in WRF_noCPM_n were poorly represented, the mean wind field components are close to observations at the times shown. At these times, there is little difference between the two different WRF simulations, although the radial flow is larger near the surface when the CPM is included. This is presumably due to the downward mixing of momentum associated with larger turbulence. WRF_CPM_n is closer to EULAG_n in representing the radial flow below the heights where observations are available. These results support previous findings that WRF is able to accurately simulate the observed

[2] The domain averaging doesn't include the initial 48 grid points by the west and south boundary in the WRF simulations. The initial 24 grid points are neglected as this is the region where random temperature perturbations are introduced by the CPM. The next 24 grid points are also neglected in order to give some spatial distance for the perturbations to develop into finer-scale turbulence.

mesoscale wind field [1].

In terms of TKE, however, WRF_noCPM_n performs quite poorly. EULAG_n performs very well in comparison to observations. In comparison to WRF_CPM_n there are larger deviation closes to the surface, where EULAG uses partial slip as lower boundary condition with a drag coefficient of 0.03 [21], and no land-use data. The TKE in WRF_noCPM_n is much lower than all other profiles. Both EULAG_n and WRF_CPM_n simulations are a vast improvement on WRF_noCPM_n at this time.

3.2. Stable case

For the stable case, on 18.11.2021, the focus is at 03:35 UTC. For this case (hereafter WRF_CPM_s) there is no equivalent WRF simulation without the CPM. As it is clear from the neutral case presented above that WRF without modifications is unable to generate realistic turbulence, it would not be worthwhile using such a large amount of computer hours to generate another very low turbulence field.

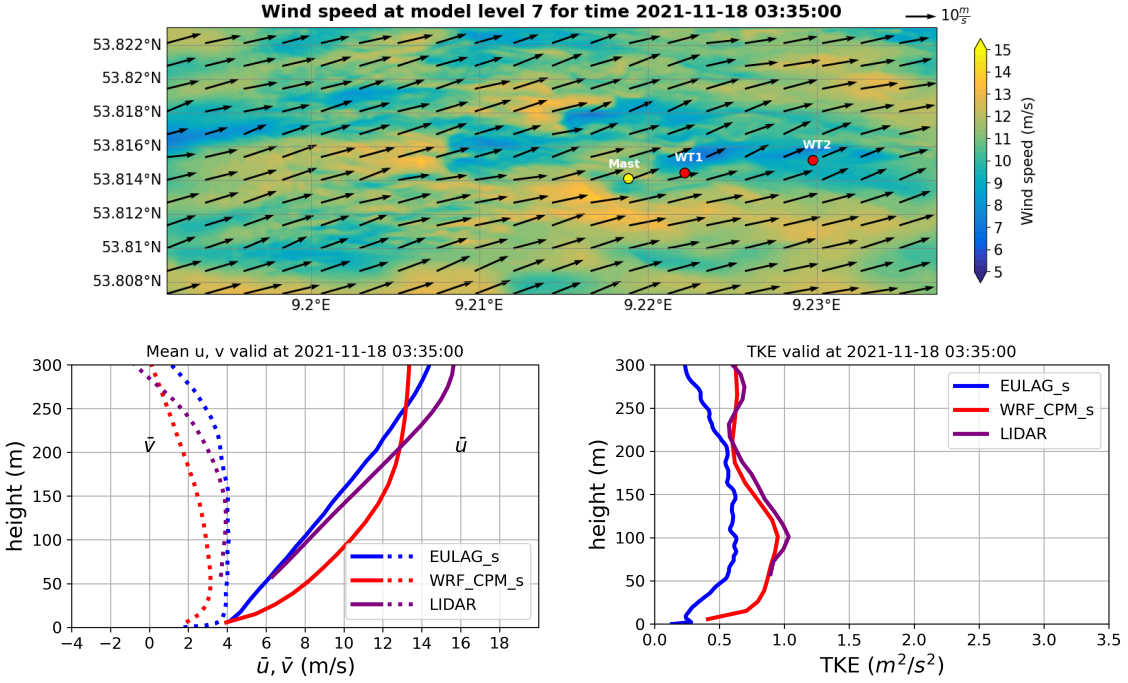

Figure 5. Horizontal cross section (top), mean horizontal velocity components (bottom left), and TKE (bottom right) as described in Figures 3-5, but for the stable case at 03:35 UTC.

Figure 5 shows the horizontal wind profile at close to 100 m (top panel), and the mean flow fields and TKE (bottom panels) at 03:35 UTC, as in the neutral case. The TKE in WRF_CPM_s is compared to a similar case in EULAG (hereafter EULAG_s) and to observations. The wind fields in EULAG_s are closer to observations than in WRF. The WRF profiles are between 1-2 m s^{-1} off observations at most heights in the boundary layer. EULAG_s lies almost directly on top of observations, a result which verifies that the assimilation technique was successful.

For the stable case the flow is, as expected, not nearly as turbulent as the neutral case presented above. WRF_CPM_s has a TKE profile that is almost identical to the observations at this time. In EULAG_s, the characteristic stably-stratified turbulence is generated in the precursor simulation. The anisotropy subgrid-scale model together with a high spacial resolution of 3 m close to the surface represents the characteristic maximum of resolved and subgrid-scale

TKE close to the surface (not shown here, see [22] Fig. 2). Including a data assimilation technique, the vertical gradient of the TKE profile becomes similar in WRF and EULAG. The general lower turbulence level in EULAG_s in comparison to WRF_CPM_s and measurements represents the mesoscale impact which is not included in the assimilated LES.

3.3. Energy Spectra

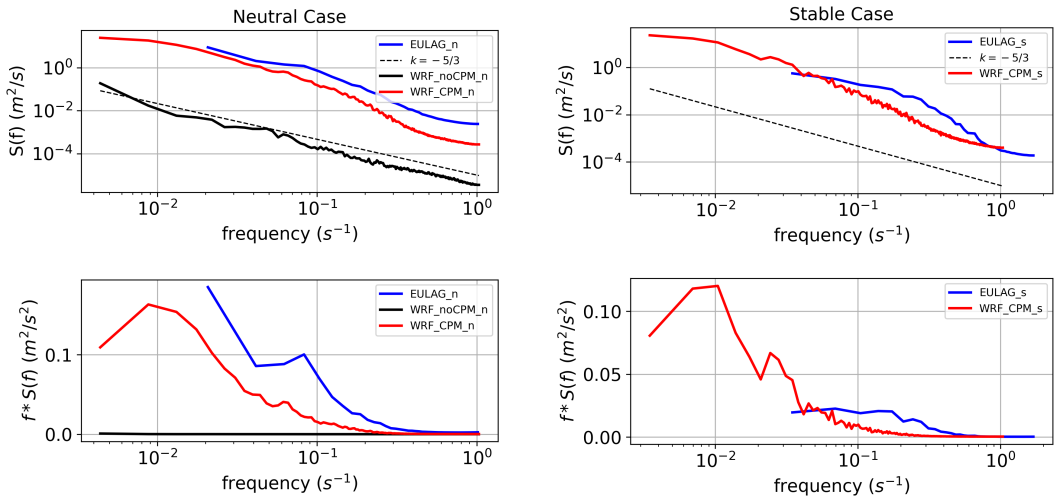

Figure 6. Energy spectra are presented for the neutral case (left) and for the stably-stratified one (right). The two rows show different representations (logarithmic y-axis in the top row, linear in the bottom row) of the spectral energy density ($S(f)$) in dependence of the frequency f. The dashed line represents the $k^{-\frac{5}{3}}$ slope, which is characteristic for the inertial subrange.

We present in Figure 6 the resolved energy spectra of u for the neutral and stable cases, with comparisons to the equivalent EULAG simulations. No comparable spectra can be reproduced from measurements. The energy spectra are taken at a height of 100 m in both models, at 18:34 UTC for the neutral case, and at 03:35 UTC for the stable case.

While all simulations have energy spectra that follow the expected $k = -5/3$ slope (top panels), there is much more energy at all frequencies in EULAG_n and WRF_CPM_n in comparison to WRF_noCPM_n under neutral conditions. WRF_CPM_n and EULAG_n include high values of low frequency energy, which are related to larger sized eddies. This statement is also valid for the stable case. In the stable case, the spectral energy density is larger in EULAG_s in comparison to WRF_CPM_s. However, EULAG_s begins to trail off at lower frequencies. In both cases the curves extend further into low frequencies for the WRF simulations, the result of a larger domain used in WRF in comparison to EULAG.

In the inertial range, both models follow the Kolmogorov spectrum. The application of a subgrid-scale model accounting for anisotropy effects in EULAG, explains the deviation from the -5/3 slope from Kolmogorov theory for high frequencies.

The CPM method adds energy both at low and high frequencies to the WRF simulation. At low frequencies (large-scale turbulence) this is especially noticeable (lower panels) where, at this time, there is a lot of energy in larger eddies when compared to WRF simulations without the CPM. A quick inspection of Figure 2 shows that this result is not surprising.

4. Conclusions

This work aims to evaluate the ability of WRF-LES to accurately reproduce realistic turbulence characteristics at a flat but heterogeneous terrain site (here: the WiValdi research park) in a quasi-neutral and stable atmospheric boundary layer. We aim to provide realistic turbulent output so that accurate wind loads and energy estimates in realistic atmospheric conditions can be produced. WRF-LES model results are compared with observations to assess qualitative and quantitative agreement, and to assess statistical model skill of TKE and energy spectra.

The results show that, while this version of WRF (V4.4.1) is capable of reproducing the mean wind fields at the WiValdi wind park, it is unable to reproduce the turbulence characteristics observed. When the CPM method to accelerate turbulent motions is included, results are significantly improved. WRF results with the CPM method included show excellent agreement with the $k = -5/3$ power law. In other words, the inertial subrange is successfully simulated with a similar energy in WRF. It is also compared to an assimilation simulation with EULAG, resulting in the same characteristic features (mean wind, TKE, spectral energy density).

In previous studies it was shown that WRF can develop realistic turbulence, albeit with a prohibitively long fetch distance [23]. Here we show that, when the CPM is applied to all LES domains, realistic turbulence develops within the relatively short times calculated here (7 h run time) and within the relatively small domain. Without the CPM, turbulence does not develop in the domain shown here.

Future research at WiValdi will allow us to analyse realistic load cases on the wind turbines and the development of wind turbine wakes (including wake interactions) with realistic inflow fields provided by WRF-LES incorporating the CPM. This work is also a first step towards a digital twin of the WiValdi research park. The recent construction of wind measurement masts array on site, once fully operational, would provide also a unique opportunity for validation of the model near the surface, which is not possible with DWL data alone (the DWL has a lowest measurement height of 57 m). The wind masts would also allow detection of the lowest forming low-level jets, which may not be captured by the DWL alone.

References

[1] Wagner J, Gerz T, Wildmann N, Gramitzky K, 2018. *Atmos. Chem. Phys.,* **19**, 1129–1146.
[2] Wise A, *et al.*, 2022. *Wind Energ. Sci.,* **7**, 367–386.
[3] Abkar M, and Portè-Agel F, 2016. *J. Phys. Conf. Ser.* **27(3)**.
[4] Vollmer L, Steinfeld G, Heinemann D, Kühn M. 2016. *Wind Energy Sci* **1**(2), 129-141.
[5] Englberger A, and Dörnbrack A, 2018. *Boundary-Layer Meteorology* **166**, 423-448.
[6] P Doubrawa, *et al.*, 2017. *J. Phys.: Conf. Ser.* 854 012010.
[7] Chow FK, Schär C, Ban N, Lundquist KA, Schlemmer L, Shi X, 2019. *Atmosphere.* 10(5):274.
[8] Muñoz-Esparza D, Kosović B, Mirocha J, *et al.*, 2014. *Boundary-Layer Meteorol* **153**, 409–440.
[9] Muñoz-Esparza B, Kosović J, van Beeck J, Mirocha, 2015. *Physics of Fluids*; **27** (3): 035102.
[10] Muñoz-Esparza D, and Kosović B, 2018. *Mon. Wea. Rev.,* **146**, 1889–1909.
[11] Wildmann N, *et al.*, 2022. *Journal of Physics: Conference Series,* **2265** (2), 022029. Institute of Physics (IOP) Publishing.
[12] Skamarock WC, *et al.*, 2008. *NCAR technical note*, Mesoscale and Microscale Meteorology Division, National Center for Atmospheric Research, Boulder, Colorado, USA.
[13] Jimenez PA, *et al.*, 2012. *Mon. Wea. Rev.,* **140**, 898–918.
[14] Niu GY, *et al.*, 2011. *Journal of Geophysical Research: Atmospheres,* **116**.
[15] Mlawer EJ, *et al.*, 1997. *J. Geophys. Res.,* **102**, 16663–16682.
[16] Dudhia J, 1989. *J. Atmos. Sci.,* **46**, 3077–3107.
[17] Hong SY, Lim JOJ, 2006. *J. Korean Meteor. Soc.,* **42**, 129–151.
[18] Kain JS, Fritsch JM, 1990. *J. Atmos. Sci.*, **47**, 2784–2802.
[19] Zhang X, Bao JW, Chen B, Grell ED, 2018. *Mon. Wea. Rev.,* **146**, 2023–2045
[20] Prusa JM, *et al.*, 2008. *Comput. Fluids* **37**.
[21] Wrba L, Englberger A, Dörnbrack A, Kilroy G, Wildmann N. *Wind Energ. Sci.,* **in review**.
[22] Wrba L, *et al.*, *Journal of Physics: Conference Series (TORQUE)* 2024, **in review**.
[23] Muñoz-Esparza D, *et al.*, 2017. *J. Adv. Model. Earth Syst.*, **9**, 1572–1594.